Transactions of the Materials Research Society of Japan 32[2] 459-463 (2007)

Blue luminescent silicon nanocrystals fabricated by microplasma jet

Tomohiro Nozaki, Kenji Sasaki, Tomohisa Ogino, Ken Okazaki
Dept of Mechanical and Control Engineering, Tokyo Institute of Technology
2-12-1 O-okayama, Meguro, Tokyo, Japan 152855
Fax: 81-3-5734-2179, e-mail: *tnozaki@mech.titech.ac.jp*

Atmospheric pressure continuous flow microplasma reactor was developed for the fabrication of silicon nanocrystals in gas phase. Mixture of argon, hydrogen, and silicon tetrachloride ($SiCl_4$) was activated by non-thermal plasma generated in a capillary glass tube with a volume of less than 1 μ-liter. A microplasma reactor provides high-density reactive media where silicon precursor is efficiently decomposed into atomic silicon even though residence time is shorter than 10-100 μs. Supersaturated silicon vapor gives rise to gas phase nucleation via three-body collision, followed by rapid termination of crystal growth due to short residence time reactor. Silicon nanocrystal is thus obtained without post annealing process. Room temperature photoluminescence (PL) excited by He-Cd laser (325 nm) exhibited intense visible emission with peak intensity around 700 nm. The PL spectrum of as-grown sample was blue-shifted down to 540 nm with increasing hydrogen content; implying nc-Si core and oxide shell structures with core diameters of 1-3 nm. Green-liminescent silicon nanocrystals blue-shifted until 450 nm after natural oxidation in air.
Key words: Microplasma, Silicon nanocrystal, Quantum confinement, Photoluminescence.

1. INTRODUCTION

Silicon nanocrystals with a grain size of less than 5 nm are widely recognized as one of the key materials in optoelectronic devices, electrodes of lithium battery, and bio-medical labels. There is also important character that silicon is safe material to the environment and easily be involved in existing silicon technologies. To date, several synthesis methods such as sputtering, laser ablation, and plasma enhanced chemical vapor deposition (PECVD) based on low-pressure processing [1-5] have been developed for precise control of size distribution of silicon nanoparticles. We explore the possibility of microplasma technologies for the efficient production of mono-dispersed nanocrystalline silicon particles in continuous flow reactor operated at atmospheric pressure [6]. Non-thermal plasmas generated in a small scale reactor is characterized as high-density non-equilibrium plasma whose electron density reaches up to ca. 10^{15} cm^{-3} [7]. Silicon precursor can be fully decomposed to create supersaturated silicon vapor which efficiently promotes nucleation of silicon nanocrystals via three-body collision; high-density plasma media is beneficial for gas phase nucleation of crystalline clusters. In addition, further growth of silicon nuclei could be avoided if residence time is shortened by microscale reactor. Giapis *et al.* has synthesized blue-luminescent silicon nanoparticles using atmospheric pressure DC hollow cathode discharge [8]. Particle size distribution was controlled by initial concentration of silane between 1 ppm and 5 ppm. Room temperature photoluminescent spectrum of as-grown particles exhibited blue emission (ca. 420 nm). Transmission electron micrograph and Raman scattering spectrum revealed that as-grown samples appeared to be coagulated amorphous silicon nanoparticles. Although authors speculate that blue-emission should originate quantum confinement of silicon nanocrystals with sizes less than 2 nm, it is not clear whether visible PL spectrum can vary from red to blue depending upon their sizes as well as surface chemistry. It is desirable if silicon nanocrystals with detailed structures such as crystal orientation and oxide layers are clearly identified and particle size distribution is correlated with plasma parameters such as electron density, gas temperature, and chemical compositions.

This paper presents the development of microplasma reactor driven by very-high-frequency power source (144 MHz) and application to silicon nanocrystal synthesis. Mixture of argon, hydrogen, and silicon tetrachloride ($SiCl_4$) was processed in this study. The particles synthesized with hydrogen less than 1% exhibited intense and stable PL spectrum with peak intensity around 700 nm. The PL intensity was enhanced by a factor of two to ten after 24-hour natural oxidation in air. The PL spectrum of as -grown sample was blue-shifted from 700 nm to 540 nm by increasing hydrogen concentration. Transmission electron micrograph clearly showed silicon nanocrystals with diameters less than 3 nm. In addition to silicon nanocrystal synthesis, fundamental plasma parameters such as electron density and excitation temperature of Ar with respect to hydrogen content is discussed.

2. EXPERIMENTAL

Figure 1 shows schematic diagram of microplasma reactor and Fig. 2 represents a close-up image of microplasma in operation. A very-high-frequency (144 MHz) power line was connected to the upper electrode via matching circuit. Microplasma is a boundary -dominated plasma, therefore high frequency operation is important to maintain high-density continuous plasma conditions. A pulsed discharge such as dielectric barrier discharge is also applicable; however, a microplasma reactor may have low throughput unless pulse duty ratio

is high enough in a short-residence time reactor. A pair of metallic electrodes was wrapped around the outside of glass capillary tube (inner diameters of 470 μm) so that contamination from electrodes into reaction zone is avoided. Argon was used as main carrier gas and a mixture of hydrogen (0-5%) and silicon tetrachloride (100-300ppm) was premixed before entering microplasma reactor. Microplasma reactor was installed in a ateel chamber in order to avoid air leak which readily oxidize as-grown samples. A 15 mm square Corning glass substrate, which was coated with chromium thin film, was located 30 mm downstream from the exit of microplasma. In addition to silicon nanocrystal synthesis, optical emission spectroscopy was performed for estimation of microplasma parameters. Emission from microplasma was introduced into a spectrometer (Spectrapro-2750, Acton research, 750 mm, 600 lines/mm) through optical fiber and data was recorded with intensified CCD camera (iDus, Andor). Electron density was estimated by Stark broadening of H_β. The excitation temperature of Ar and rotational temperature of CH were estimated from Boltzmann plot method, respectively.

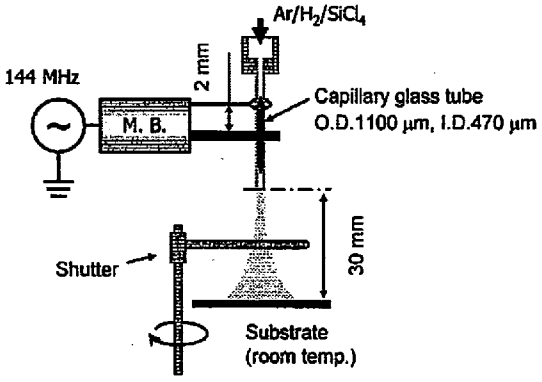

Fig. 1 Schematic diagram of microplasma reactor

3. RESULTS AND DISCUSSION

3.1. Characterization microplasma by OES

Fundamental characters of microplasma were evaluated by optical emission spectroscopy (OES). Rotational spectrum from molecular hydrogen such as G-B band and Fulcher band has been well investigated and frequently analyzed for rotational temperature of discharge plasma. However, these molecular spectra were interestingly absent in the microplasma. Therefore we added trace amount of methane for analysis of rotational temperature of CH (432 nm) that reasonably reflects gas temperature of corresponding emission region [9-10]. Note that methane was not injected into the microplasma during synthesis of silicon nanocrystals. Electron number density was estimated from Stark broadening of H_β line (486 nm) [11]. Excitation temperature of Ar was estimated from the relative intensity ration of Ar emission lines.

Figure 3 shows emission spectrum of microplasma observed between metallic electrodes as designated point A in Fig. 2. Figure 3 shows strong emission from atomic silicon near 250.7–252.9 nm, 288.2 nm, and 390.6 nm. It also shows relatively strong emission of SiCl around 300 nm when H_2 = 0%, but SiCl emission almost disappeared when H_2 = 3%. Decrease in emission intensity of SiCl implies that silicon tetrachloride decomposes not only by electron impact, but also dechlorination reaction by active hydrogen:

$$SiCl_4 + e \leftrightarrow Si + 2Cl_2 + e \qquad (R1)$$

$$SiCl_4 + H \rightarrow SiCl_n + (4\text{-}n)HCl \qquad (R2)$$

Figure 4 presents electron density (N_e), Ar excitation temperature (T_{ex}), and CH rotational temperature (T_{rot}) with respect to initial hydrogen concentration. Excitation temperature (T_{ex}) and rotational temperature (T_{rot}) were 8000 K and 1400 K, respectively with minimum amount of hydrogen content. The difference between plasma temperatures become smaller as hydrogen content increases, and finally reached 5400 K and 2100 K at H_2 = 3%. It should be noted that emission spectrum shown in Fig. 3 also exhibits continuous spectrum around 300-400 nm which attributes to vibrationlly excited hydrogen molecules. Electron energy is distributed to vibrational state of hydrogen which in turn increases translational energy of molecules via three-body collision. Electron density also declines with hydrogen concentration. Although hydrogen plays an essential role for decomposition of $SiCl_4$ as well as particle nucleation, excess amount of hydrogen turned out to be not beneficial to maintain microplasma activity.

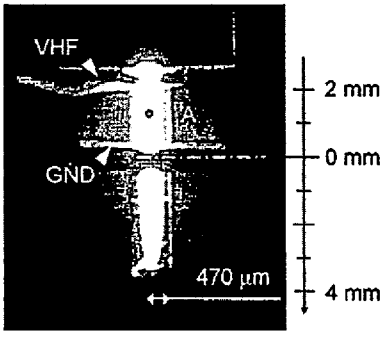

Fig. 2 A close-up image of microplasma reactor

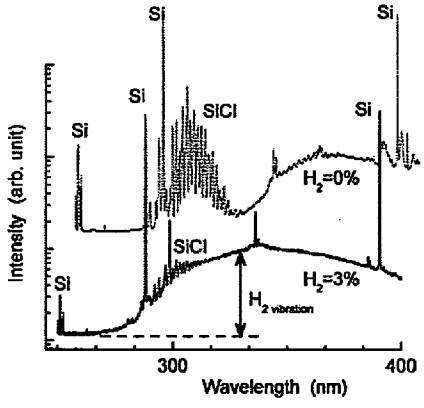

Fig. 3 Emission spectrum of microplasma. Ar: 200 cm^3 min^{-1}, $SiCl_4$: 100 ppm, Power: 35 W.

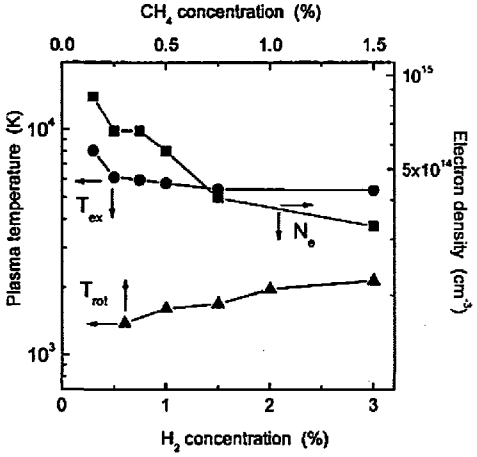

Fig. 4 Dependence of plasma parameters on hydrogen concentration (T_{ex}: Ar excitation temperature, T_{rot}: CH Rotational temperature, N_e: electron number density)

3.2. Deposition of silicon nanocrystals

Figure 5 shows electron scanning micrographs (S-800, HITACHI) of as-grown samples when hydrogen concentration was (a) 0% and (b) 3%. Deposition rate at $H_2 = 0$ was considerably slow because silicon cluster etching by chlorine, or reverse reaction of (R1), limits silicon monomer concentration. Transmission electron micrograph shown in Fig. 6 (a) reveals that the thin film actually consists of a-Si or SiO_X nanoparticles. On the other hand, deposition rate dramatically increased by adding hydrogen. A cross-section view of SEM image showed dense powder-like film which was deposited much faster than the sample without hydrogen (Fig. 5(a)). The TEM micrograph clearly shows isolated crystalline particles with grain sizes less than 3 nm. Hydrogen promotes chlorine abstraction from $SiCl_x$ and contributes to create supersaturated Si vapor condition which efficiently promotes crystal grain nucleation [3]. Upon cluster nucleation, hydrogen would terminate dangling bond of silicon cluster surfaces. This corresponds to the reduction of critical nuclei size because surface energy of silicon clusters decreases as terminated by hydrogen. In order to correlate the hydrogen concentration with silicon crystal size, photoluminescence of as-grown samples was analyzed.

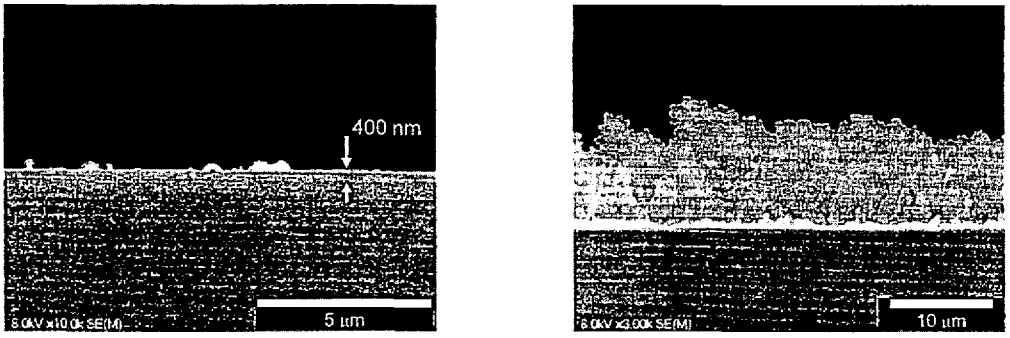

(a) H_2: 0% (b) H_2: 3%

Fig. 5 Coss-section SEM images of as-grown deposits. Ar flow rate: 200 cm_3 min_{-1}, $SiCl_4$: 100 ppm, Power: 35 W.

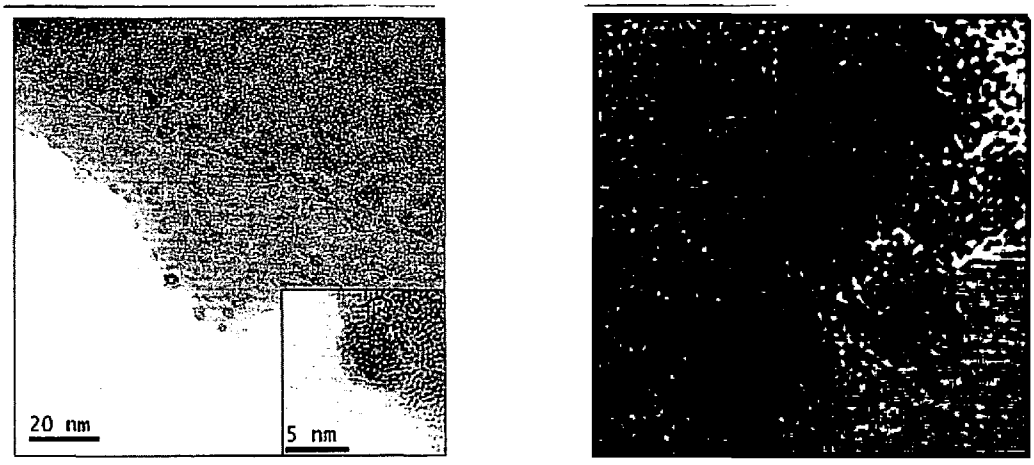

(a) H_2: 0% (b) H_2: 3%

Fig. 6 High-resolution TEM micrographs showing isolated silicon nanoparticles (a) a-Si and (b) nc-Si. Experimental conditions: see Fig. 5.

3.3. Band gap energy of silicon nanocrystals

Band gap energy of silicon nanocrystals is larger than that of bulk silicon (1.1 eV), and should increase as crystal grain size decreases. In order to estimate band gap energy of as-grown silicon nanocrystals, room temperature photoluminescent measurement was performed. A He-Cd laser (325 nm) was used as excitation light source and irradiated with incident angle of 60° from normal to the substrate. Visible photoluminescence was recorded from normal direction using the same optical setup described in section 2. Scattered laser light was eliminated by UV-cut filter that transmits longer wavelength than 370 nm (50% transmittance at 385 nm).

Figure 7 represents hydrogen-dependent changes in room temperature PL spectrum of as-grown samples. Faint visible emission was obtained between H_2 = 0% and 0.5%. The PL intensity abruptly increased when H_2 = 0.7% with peak intensity around 685 nm. The PL spectrum slightly blue-shifted as hydrogen increases, while PL intensity sharply drops. Visible PL emission between 550 nm and 650 nm was absent independently of hydrogen concentration, however green-emitting nanocrystals with peak intensity around 540 nm appeared when H_2 = 3% and 5%.

By focusing on maximum PL intensity and corresponding wavelength, PL spectra provided in Fig. 7 are re-plotted in Fig. 8. The results clearly show that the peak wavelength monotonically decreases with hydrogen and reaches constant value around 540 nm. If silicon particle is perfectly terminated by hydrogen, band gap energy should exponentially increase with decreasing crystal grain size; however, in the actual situation, particle must be more or less oxidized after exposure to air: band gap energy is a strong function of surface status rather than grain size. Luppi *et al.* [12] estimated relationship between band gap energy and number of surface oxide states, suggested that even a single silicon atom is doubly terminated by oxygen (Si=O), band gap energy only slightly increases with decreasing crystal grain size and finally reaches saturated value around 2.25 eV. Peak wavelength of

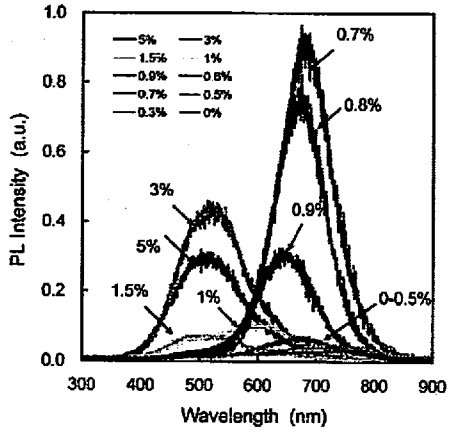

Fig. 7 Hydrogen dependent changes in PL spectrum. Ar: 200 cm^3 min^{-1}, $SiCl_4$: 100 ppm, Power: 35 W, synthesis time: 3 min for H_2 = 0-1%, and 15 min for H_2 = 1.5%-3%, respectively.

green-luminescent silicon nanocrystals (540 nm = 2.3 eV) shown in Fig. 8 is well correlated with numerical and experimental estimation [12-13]. Hydrogen influences not only plasma parameters, but also reaction pathways and crystal nucleation rate; however, changes in plasma parameters may have a small effect because electron density (N_e) and plasma temperatures (T_{ex} and T_{rot}) only monotonically changes with respect to hydrogen concentration. As discussed in 2.2, crystal grain size may decrease if silicon cluster surface is covered by hydrogen since surface energy efficiently decreases. The same trend is observed when $SiCl_4$ concentration was varied. The PL spectrum shown in Fig. 9 slightly blue-shifted when $H_2/SiCl_4$ ratio increased.

3.4. Natural oxidation of as-grown silicon nanocrystals

In general, PL intensity of as-grown sample increases as it is oxidized [14]. As shown in Fig. 10, PL intensity of red-luminescent sample clearly increases as it is oxidized, however peak wavelength is not influenced by natural oxidation. The enhancement factor for PL intensity varied from two to ten depending on samples, but oxidation process seems to reach steady state in 24-hour. Formation of oxide shell probably works as radiative recombination center of electron-hole pair [14].

Oxidation of green-luminescent sample showed a different trend as shown in Fig. 11. The PL intensity remarkably decreased while spectrum blue-shifted as oxidation proceeds. Characterization of blue-luminescent silicon nanocrystals is problematic because predicted maximum band gap energy of oxygen terminated silicon nanocrystals would be 2.5 eV (~500 nm) with crystal grain sizes between 0.5 nm and 1.0 nm [12]. Nevertheless, we speculate that the presence of silicon nanocrystals is responsible for blue emission. The nc-Si core may shrink as its surface is oxidized, and thus PL spectrum blue-shifts.

4. CONCLUDING REMARKS

An atmospheric pressure, continuous-flow microplasma reactor was developed for deposition of silicon nanocrystal containing thin film. In addition to electron impact dissociation of $SiCl_4$, hydrogen

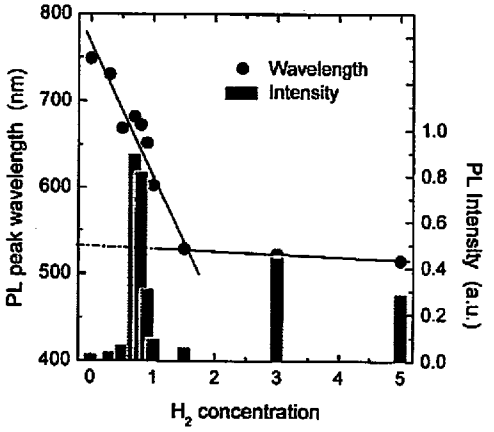

Fig. 8 Effect of hydrogen concentration on band gap energy and PL intensity. conditions see Fig. 7.

promotes dechlorination reaction of $SiCl_x$ and contributes to increase silicon monomer concentration. Upon particle nucleation, hydrogen would passivate crystalline cluster surfaces and decreases critical cluster size: hydrogen contributes to decrease crystal grain size. Room temperature photoluminescence (PL) exhibited intense visible light emission with the peak intensity around 700 nm when H_2 = 0.7%. The PL spectrum blue-shifted as $H_2/SiCl_4$ ratio increases, and finally saturated around 540 nm. This tendency quite well correlated with experimental and numerical predictions, suggesting that as-grown sample has nanocrystalline core and oxide shell structures with core sizes between 1 nm and 3 nm. Further increase in hydrogen does not contribute to blue-shift below 540 nm, however, green-luminescent particles (PL wavelength = 540 nm) blue-shifted until 450 nm after natural oxidation in air for 24-hour because nanocrystalline core shrinks after forming oxide shell. As for PL intensity of red-luminescent silicon nanocrystals, there is a unique dependence on hydrogen concentration. The role of hydrogen on nanocrystal formation must be further investigated.

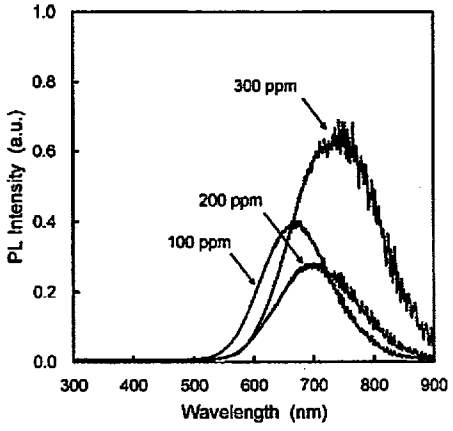

Fig. 9 Changes in peak location with respect to initial $H_2/SiCl_4$ ratio. Ar: 200 cm^3 min^{-1}, H_2: 0.7%, Power: 35 W, as-grown samples.

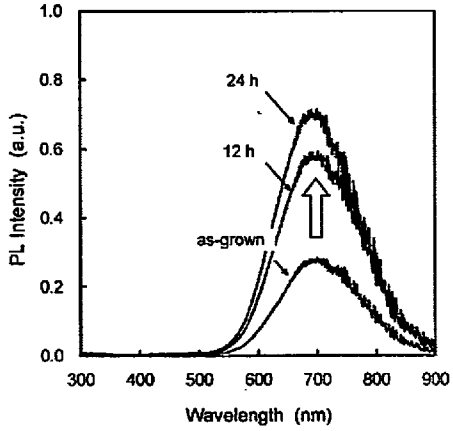

Fig. 10 Enhancement of PL intensity after natural oxidation in air. Spectrum peak position remained unchanged. Ar: 200 cm^3 min^{-1}, H_2: 0.7%, $SiCl_4$: 200 ppm, Power: 35 W.

Acknowledgement

This project was supported by the Grants-in-Aid for Scientific Research on the Priority Area of Microplasmas from the Japanese Ministry of Education, Culture, Sports, Science and Technology. Mr. Akira Genseki, Center for Advanced Materials Analysis of Tokyo Institute of Technology, supported TEM analysis. T.N. would like to thank Professor Hajime Shirai, Saitama University, for intensive discussion of material characterization.

References

[1] T. Makimura, T. Mizuta and K. Murakami, *Jpn. J. Appl. Phys.*, 41, L144-L146 (2002).
[2] L. Xuegeng, H. Yuanqing, S. S. Talukdar, M. T. Swihart, *Langmuir*, 19 8490-8496 (2003).
[3] S. L. Girshick, N. P. Rao, M. Kelkar, *J. Vac. Sci. Technol. A*, 14(2) 529-534 (1996).
[4] L. Mangolini, E. Thimsen, U. Kortshagen, *NANO LETTERS*, 5(4) 655-659 (2005).
[5] T. Kakeya, K. Koga, M. Shiratani, Y. Watanabe, M. Kondo, *Thin Solid Films*, 506 507 288-291 (2006).
[6] http://plasma.kuee.kyoto-u.ac.jp/tokutei429/
[7] T. Ichiki, R Taura, Y. Horiike, *J. Appl. Phys.*, 95(1), 35 (2004).
[8] R. M Sankaran, D. Holunga, R. C. Flagan, K. P. Giapis, *NANO LETTERS*, 5(3), 537-541 (2005).
[9] T. Nozaki, Y. Miyazaki, Y. Unno and K. Okazaki, *J. Phys. D: Appl. Phys.*, 34, 3383 (2001).
[10] T. Nozaki, Y. Unno and K. Okazaki, *Plasma Sources Sci. Technol.*, 11, 431 (2002).
[11] H. R. Griem, "Plasma Spectroscopy", McGraw-Hill, New York, (1964).
[12] M. Luppi, S. Ossicini, *J. Appl. Phys.*, 94 2130-2132 (2003).
[13] M. V. Wolkinm J. Jorne, P. M. Fauchet, *Phys. Rev. Lett.*, 82(1) 197-200 (1999).
[14] Y. Hirano, F. Sato, N. Saito, M. Abe, S. Miyazaki, M. Hirose, *J. Non-cys. Solid.*, 266-269 1004-1008 (2000).

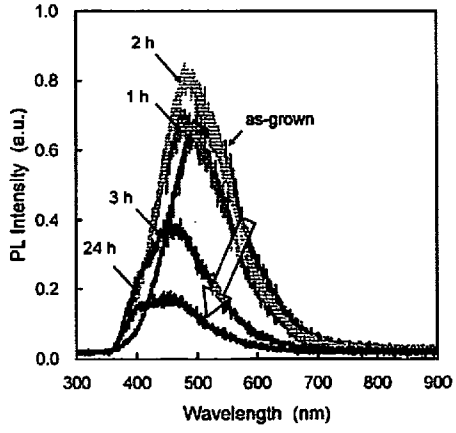

Fig. 11 Time-dependent changes in PL intensity of green-luminescent silicon nanocrystlas during natural oxidation. Ar: 200 cm^3 min^{-1}, H_2: #%, $SiCl_4$: 100 ppm, Power: 35 W.

(Received December 14, 2006;Accepted December 26, 2006)